An Auto-Calibration Method for Unattended Ground Sensors

Randolph L. Moses, Dushyanth Krishnamurthy, and Robert Patterson

Department of Electrical Engineering, The Ohio State University
2015 Neil Avenue, Columbus, OH 43210 USA

Abstract

We present an algorithm for locating and orienting a set of sensor arrays that have been deployed in a scene at unknown locations and orientation angles. This self-calibration problem is solved using a number of source signals also deployed in the scene. We assume each array can estimate the time-of-arrival and direction-of-arrival (with respect to the array's local orientation coordinates) of every source. From this information we compute the array locations and orientations. We consider four subproblems, in which the source signals or emission times are either known or unknown. We develop necessary conditions for solving the self-calibration problem and provide a maximum likelihood solution and corresponding location error estimate.

1. Introduction

Unattended Ground Sensors (UGSs) are becoming increasingly important for providing situational awareness in battlefield deployments [1]. The basic concept is to deploy a large number of low-cost, self-powered sensors that acquire and process data. The sensors typically consist of an array of microphones to detect, track, and classify acoustic signatures. In addition, seismic and low-cost imaging sensors may also be present.

We consider a sensor deployment architecture as shown in Figure 1. A number of low-cost sensors, each equipped with a local processor, a low-power communication transceiver, and one or more sensing capabilities, is set out in a region. Sensor elements may collect acoustic, seismic, and/or image data. Each sensor monitors its environment to detect, track, and characterize signatures. The sensed data is processed locally, and the result is transmitted to a local Central Information Processor (CIP) through a low-power communication network. The CIP fuses sensor information and transmits the processed information to a more distant command center.

In order to fuse sensor information at the CIP or command center, it is important to know the location and orientation of each sensor. Ground sensors are placed in the field by persons, by an air drop, or by artillery

Report Documentation Page

Report Date	Report Type	Dates Covered (from... to)
00 Oct 2001	N/A	-

Title and Subtitle An Auto-Calibration Method for Unattended Ground Sensors	**Contract Number**
	Grant Number
	Program Element Number
Author(s)	**Project Number**
	Task Number
	Work Unit Number
Performing Organization Name(s) and Address(es) The Ohio State University Department of Electrical Engineering 2015 Neil Avenue Columbus, OH 43210	**Performing Organization Report Number**
Sponsoring/Monitoring Agency Name(s) and Address(es) Department of the Army, CECOM RDEC Night Vision & Electronic Sensors Directorate AMSEL-RD-NV-D 10221 Burbeck Road Ft. Belvoir, VA 22060-5806	**Sponsor/Monitor's Acronym(s)**
	Sponsor/Monitor's Report Number(s)

Distribution/Availability Statement
Approved for public release, distribution unlimited

Supplementary Notes
See also ADM201471, Papers from the Meeting of the MSS Specialty Group on Battlefield Acoustic and Seismic Sensing, Magnetic and Electric Field Sensors (2001) Held in Applied Physics Lab, Johns Hopkins Univ, Laurel, MD on 24-26 Oct 2001. Volume 2 (Also includes 1999 and 2000 Meetings), The original document contains color images.

Abstract

Subject Terms

Report Classification unclassified	**Classification of this page** unclassified
Classification of Abstract unclassified	**Limitation of Abstract** UU

Number of Pages
14

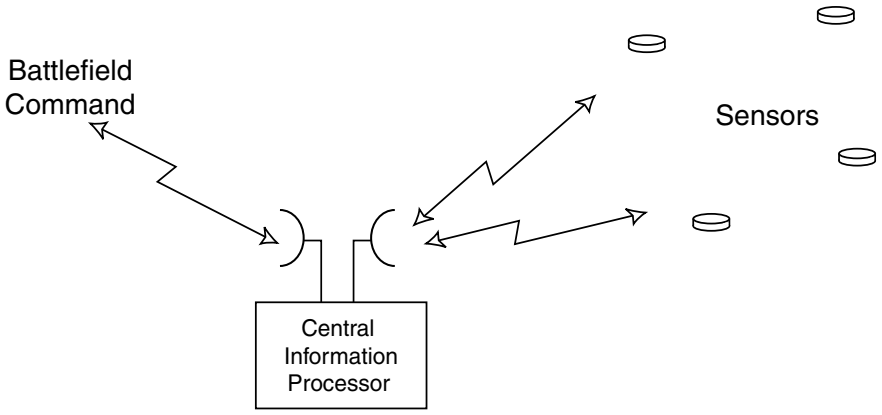

Figure 1: Sensor network architecture. A number of low-cost sensors are deployed in a region. Each sensor communicates to a local CIP, which relays information to a more distant command center.

launch. For careful hand placement, accurate location and orientation of the sensors can be assumed; however, for many sensor deployment situations, it is difficult or impossible to know accurately the location and orientation of each sensor. One could equip each sensor with a GPS and compass to obtain location and orientation information, but this adds to the expense and power requirements of the sensor and may increase susceptibility to jamming. Thus, there is interest in developing methods to self-calibrate the sensor array with a minimum of additional hardware or processing.

In this paper we consider an approach to array self-calibration using sources in the field. A number of signal sources are deployed in the same region as the sensors (see Figure 2). Each source generates a unique signature that is detected by the sensors. From the time-of-arrival (TOA) and direction-of-arrival (DOA) of each source signal, we compute the unknown locations and orientations of the sensors. We consider four related subproblems, in which:

1. the source locations and emission times are known,
2. the source locations are known and emission times are unknown,
3. the source locations are unknown and emission times are known,
4. the source locations and emission times are unknown.

Several researchers have considered the problem of array calibration, but less work is devoted to calibrating networks of sensors. A number of papers have considered calibration of both narrowband and broadband arrays of sensors to improve direction-of-arrival estimation accuracy [2, 3, 4, 5, 6, 7]. These papers assume knowledge of the nominal sensor locations high (or perfect) signal coherence between the sensors. Calibration requirements for acoustic ground sensors are discussed in [8]. Research on blind beamforming considers a related problem of forming a maximum power beam to a source without computing the source locations [9]. A recent paper considers sensor self-calibration using a single acoustic source that travels in a straight line [10].

An outline of the paper is as follows. In Section 2 we present a statement of the problem and justify our assumptions. In Section 3 we first consider necessary conditions for a self-calibration solution and present

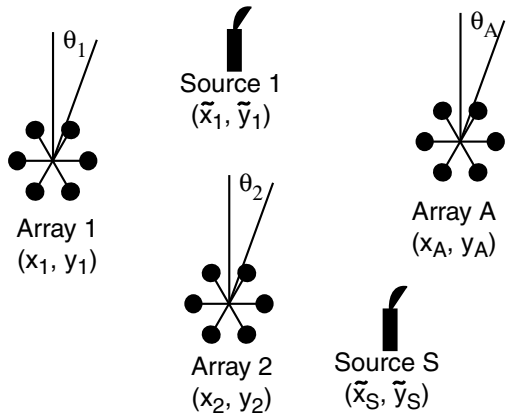

Figure 2: Array self-calibration scenario.

methods for solving the self-calibration problem with a minimum number of sensors and sources. These methods provide initial estimates for an iterative descent computation needed to obtain maximum likelihood calibration parameter estimates derived in Section 4. Bounds on the calibration uncertainty are also derived. Section 5 presents numerical examples to illustrate the approach, and Section 6 presents conclusions and directions for future work.

2. The Self-Calibration Problem

Assume we have a set of A sensors, each with unknown location $\{a_i = (x_i, y_i)\}_{i=1}^{A}$ and unknown orientation angle θ_i with respect to a reference direction (*e.g.*, North). We consider the two-dimensional problem in which the sensors lie in a plane and the unknown reference direction is azimuth; an extension to the three-dimensional case is possible using similar techniques.

In the array field are also placed S point source signals at locations $\{s_j = (\tilde{x}_j, \tilde{y}_j)\}_{j=1}^{S}$. The source locations may be known or unknown. Each source emits a finite-length signal that begins at time t_j; the emission times may be known or unknown. We thus consider four related subproblems, depending on the prior knowledge of the source locations and their emission times.

We initially assume each emitted source signal is detected by all of the sensors in the field (the extension to partial measurements is considered in Section 4.4) and that each sensor measures the time-of-arrival (TOA) and direction-of-arrival (DOA) for that source. We denote the measured TOA of source j to sensor i as t_{ij} and the measured DOA as θ_{ij}.

The DOA measurements are made with respect to a local (to the sensor) frame of reference. The absolute directions of arrival are not available because the orientation angle of each array is unknown (and must be estimated in the calibration procedure). The times of arrival are measured with respect to a known, common time base. The time base can be established either by using the electronic communication network linking the sensors or by synchronizing the sensor processor clocks before deployment. The time base needs to be accurate to a number on the order of the sensor's time of arrival measurement uncertainty (1 msec in the

examples in Section 5).

The set of $2AS$ measurements are gathered in a vector

$$X = \left[\begin{array}{c} \mathrm{vec}(T) \\ \mathrm{vec}(\Theta) \end{array} \right]^T \quad (2AS \times 1) \tag{1}$$

where $\mathrm{vec}(M)$ stacks the elements of a matrix M columnwise and where

$$T = \left[\begin{array}{cccc} t_{11} & t_{12} & \dots & t_{1S} \\ t_{21} & t_{22} & \dots & t_{2S} \\ \vdots & \vdots & \ddots & \vdots \\ t_{A1} & t_{A2} & \dots & t_{AS} \end{array} \right], \qquad \Theta = \left[\begin{array}{cccc} \theta_{11} & \theta_{12} & \dots & \theta_{1S} \\ \theta_{21} & \theta_{22} & \dots & \theta_{2S} \\ \vdots & \vdots & \ddots & \vdots \\ \theta_{A1} & \theta_{A2} & \dots & \theta_{AS} \end{array} \right] \tag{2}$$

Each array transmits its $2S$ TOA and DOA measurements to a central information processor, and these $2AS$ measurements form the data with which the CIP computes the array calibration. Note that the communication cost to the CIP is low, and the calibration processing is entirely performed by the CIP.

Define the parameter vectors

$$\alpha = [\beta^T, \gamma^T]^T \quad (3(A+S) \times 1) \tag{3}$$
$$\beta = [x_1,\, y_1,\, \theta_1, \dots, x_A,\, y_A,\, \theta_A]^T \quad (3A \times 1) \tag{4}$$
$$\gamma = [\tilde{x}_1,\, \tilde{y}_1,\, t_1, \dots, \tilde{x}_S,\, \tilde{y}_S,\, t_S]^T \quad (3S \times 1) \tag{5}$$

We denote the actual TOA and DOA of source signal j at sensor i as $\tau_{ij}(\alpha)$ and $\phi_{ij}(\alpha)$, respectively, and include their dependence on the parameter vector α; they are computed as:

$$\tau_{ij}(\alpha) = t_j + \|a_i - s_j\|/c \tag{6}$$
$$\phi_{ij}(\alpha) = \theta_i + \angle(a_i, s_j) \tag{7}$$

where $\|\cdot\|$ is the Euclidean norm, $\angle(\xi, \eta)$ is the angle between the points $\xi, \eta \in \mathcal{R}^2$, and c is the signal propagation velocity.

Each element of X has measurement uncertainty; we model the uncertainty as

$$X = \mu(\alpha) + E \tag{8}$$

where $\mu(\alpha)$ is the noiseless measurement vector whose elements are given by equations (6) and (7) for values of i, j that correspond to the vector stacking operation in (1), and where E is a random vector with known probability density function.

The self-calibration problem, then, is given the measurement X, estimate β. Note that none, some, or all of the parameters in γ may be known depending on the particular subproblem of interest.

3. Existence and Uniqueness of Solutions

In this section we address the existence and uniqueness of solutions to the self-calibration problem and establish the minimum number of sensors and sources needed to obtain a solution. We assume that every sensor detects every source and measures both TOA and DOA. In addition, we assume the TOA and DOA measurements are noiseless. We establish the minimum number of sources and sensors needed to compute a unique calibration solution and give algorithms for finding the self-calibration solution in the minimal cases. These algorithms provide initial estimates to an iterative descent algorithm for the practical case of non-minimal, noisy measurements presented in Section 4.

The four cases below make different assumptions about the source signal parameters. In all four cases the number of measurements is $2AS$, and determination of β involves solving a nonlinear set of equations for its $3A$ unknowns. Depending on the case considered, we may also need to estimate the unknown nuisance parameters in γ. The result in each case is summarized in Table 1.

Case 1: Known source locations and emission times.

A unique solution for β can be found for any number of sensors as long as there are $S \geq 2$ sources. In fact, the location and orientation of each sensor can be computed independently of other sensor measurements. The location of the ith sensor, a_i, is found from the intersection of two circles with centers at the source locations and with radii $(t_{i1} - t_2)/c$ and $(t_{i2} - t_1)/c$. The intersection is in general two points; the correct location can be found using the sign of $\theta_{i2} - \theta_{i1}$. We note that the two circle intersections can be computed in closed-form. From the known source and sensor locations and the DOA measurements, the sensor orientations can also be uniquely found.

Case 2: Known source locations, unknown emission times.

For $S \geq 3$ sources the location and orientation of each sensor can be computed in closed form independently of other sensors. A solution procedure is as follows. Consider the pair of sources (s_1, s_2). Sensor i knows the angle $\theta_{i2} - \theta_{i1}$ between these two sources. The set of all possible locations for sensor i is an arc of a circle whose center and radius can be computed from the source locations (see Figure 3). Similarly, a second circular arc is obtained from the source pair (s_1, s_3). The intersection of these two arcs is a unique point and can be computed in closed form. Once the sensor location is known, its orientation is readily computed from any of the three DOA measurements.

A solution for Case 2 can also be found using $S = 2$ sources and $A = 2$ sensors. The solution requires a one-dimensional search of a parameter over an finite interval. The known location of s_1 and s_2 and the known angle $\theta_{11} - \theta_{12}$ means that array a_1 must lie on a known circular arc as in Figure 3. Each location along the arc determines both source emission times. At exactly one position along the arc, the emission times are consistent with the measurements from the second sensor.

Table 1: Minimal Solutions for Array Self-Calibration

Case	# Unknowns	Minimum $A,\ S$	Comments
Known Locations Known Times	$3A$	$A = 1,\ S = 2$	closed-form solution
Known Locations	$3A + S$	$A = 1,\ S = 3$	closed-form solution
Unknown Times	$3A + S$	$A = 2,\ S = 2$	1-D iterative solution
Unknown Locations Known Times	$3(A-1) + 2S$	$A = 2,\ S = 2$	closed-form solution
Unknown Locations Unknown Times	$3(A + S - 1)$	$A = 2,\ S = 3$ or $A = 3,\ S = 2$	2-D iterative solution

Case 3: Unknown source locations, known emission times.

In this case and in Case 4 below, the calibration problem can only be solved to within an unknown translation and rotation of the entire sensor-source scene because any translation or rotation of the entire scene does not change the t_{ij} and θij measurements. To eliminate this ambiguity, we assume the location and orientation of the first sensor are known; without loss of generality we set $x_1 = y_1 = \theta_1 = 0$. We solve for the remaining $3(A-1)$ parameters in β.

For the case of unknown source locations, a unique solution for β is computable in closed form for $S = 2$ and any $A \geq 2$ (the case $A = 1$ is trivial). From sensor a_1 the range to each source can be computed from $r_j = (t_{1j} - t_j)/c$, and its bearing is known, so the locations of the two sources can be found. The locations and orientations of the remaining sensors is then computed using the method of Case 1.

Case 4: Unknown source locations and emission times.

For this case it can be shown that an infinite number of calibration solutions exists for $A = S = 2$,[1] but that a unique solution exists in almost all cases for either $A = 2,\ S = 3$ or $A = 3,\ S = 2$. In some degenerate cases, not all of the γ parameters can be uniquely determined, although we do not know of a case for which the β parameters cannot be uniquely found.

Closed-form calibration solutions are not known for this case, but solutions that require a two-dimensional search can be found. We outline one such solution that works for either $A = 2$ and $S \geq 3$ or $S = 2$ and $A \geq 3$. Assume as before that sensor a_1 is at location $(x_1, y_1) = (0, 0)$ with orientation $\theta_1 = 0$. If we knew the two source emission times t_1 and t_2, we can find the locations of sources s_1 and s_2 as in Case 3. From the two known source locations, all remaining sensor locations and orientations can be found using the procedure in Case 1, and then all remaining source locations can be found using triangulation from the known arrival angles and known sensor locations. The solutions will be inconsistent except for the correct values of t_1 and t_2. The calibration procedure, then, is to iteratively adjust t_1 and t_2 to minimize the error

[1] Note that for $A = S = 2$ there are 8 measurements and 9 unknown parameters. The set of possible solutions in general lies on a one-dimensional manifold in the 9-dimensional parameter space.

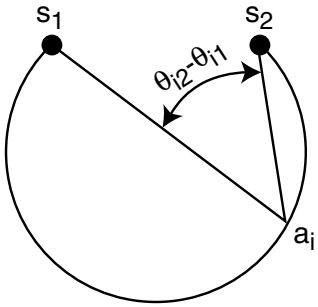

Figure 3: A circular arc is the locus of possible sensor locations whose angle between two known points is constant.

between computed and measured time delays and arrival angles.

4. Maximum Likelihood Self-Calibration

In this section we derive a maximum likelihood (ML) estimator for the unknown array location and orientation parameters. The algorithm involves the solution of a set of nonlinear equations for the unknown parameters (and the unknown nuisance parameters in γ). The solution is found by iterative minimization of a cost function; we use the methods in Section 3 to initialize the iterative descent. In addition, we derive the Cramer-Rao Bound (CRB) for the variance of the unknown parameters in α; the CRB also gives high-SNR parameter variance of the ML parameter estimates.

4.1 The Maximum Likelihood Estimate

We assume the measurement uncertainty E in equation (8) is Gaussian with zero mean and known covariance Σ. In this case the likelihood function is

$$f(X;\alpha) = \frac{1}{(2\pi\sigma_t\sigma_\theta)^{AS}} \exp\left\{-\frac{1}{2}Q(X;\alpha)\right\} \tag{9}$$

$$Q(X;\alpha) = [X-\mu(\alpha)]^T\Sigma^{-1}[X-\mu(\alpha)] \tag{10}$$

A special case is when the measurement errors are uncorrelated and the TOA and DOA measurement errors are Gaussian with zero mean and variances σ_t^2 and σ_θ^2, respectively; then equation (10) becomes

$$Q(X;\alpha) = \sum_{i=1}^{A}\sum_{j=1}^{S}\left[\frac{(t_{ij}-\tau_{ij}(\alpha))^2}{\sigma_t^2} + \frac{(\theta_{ij}-\phi_{ij}(\alpha))^2}{\sigma_\theta^2}\right] \tag{11}$$

In the four cases considered in Section 3, some of the parameters in α are known. We denote α_1 to be the unknown parameters in α and α_2 to be the known parameters for the particular case of interest. Using this

notation along with equation (9), the maximum likelihood estimate of α_1 is

$$\hat{\alpha}_{1,ML} = \arg\max_{\alpha_1} f(X, \alpha_2; \alpha) = \arg\min_{\alpha_1} Q(X; \alpha) \tag{12}$$

4.2 Nonlinear Least Squares Solution

The solution of (12) involves solving a nonlinear least squares problem. A standard iterative descent procedure can be used, initialized using one of the solutions in Section 3. In our implementation we used the Matlab function `lsqnonlin`.

The straightforward nonlinear least squares solution we adopted converged quickly (in several seconds for all examples tested) and displayed no symptoms of numerical instability; however, alternative methods for solving equation (12) may reduce computation. One can divide the parameter set and iterate first on the sensor location parameters and second on the remaining parameters. Although the sensor orientations and source parameters depend nonlinearly on the sensor locations, computationally efficient approximations exist (see, *e.g.*, [11]), so the computational savings of lower dimensional searches may exceed the added computational cost of iterations nested in iterations if the methods are tuned appropriately. Similarly, one can view the source parameters as nuisance parameters and employ estimate-maximize (EM) algorithms to obtain the ML solution [12].

4.3 Estimation Accuracy

The Cramer-Rao Bound (CRB) gives a lower bound on the covariance of any unbiased estimate of α_1. It is a tight bound in the sense that $\hat{\alpha}_{1,ML}$ has parameter uncertainty given by the CRB for high signal-to-noise ratio; that is, as $\max_i \Sigma_{ii} \to 0$. Thus, the CRB is a useful tool for analyzing calibration uncertainty.

The CRB can be computed from the Fisher Information Matrix of α_1. The Fisher Information Matrix is given by [13]

$$I_{\alpha_1} = E\left\{ \left[\nabla_{\alpha_1} \ln f(T, \Theta; \alpha)\right] \left[\nabla_{\alpha_1} \ln f(T, \Theta; \alpha)\right]^T \right\}$$

The partial derivatives are readily computed from equations (9), (6), and (7); we find that

$$I_{\alpha_1} = [G'(\alpha_1)]^T \Sigma^{-1} [G'(\alpha_1)] \tag{13}$$

where $G'(\alpha_1)$ is the $2AS \times \dim(\alpha_1)$ matrix whose ijth element is $\partial \mu_i(\alpha_1)/\partial(\alpha_1)_j$.

For Cases 3 and 4, the Fisher information matrix is rank deficient due to the translational and rotational ambiguity in the self-calibration solution in those two cases. In this situation, two approaches can be taken.

First, one can assume some of the sensor parameters are known. Examples are to assume known location and orientation of a single sensor, or to assume known location of two sensors. These assumptions might be realized by equipping one sensor with a GPS and a compass, or by equipping two sensors with GPSs. Let $\tilde{\alpha}_1$ denote the vector obtained by removing these assumed known parameters from α_1. To compute the CRB matrix for $\tilde{\alpha}_1$ in this case, we first remove all rows and columns in I_{α_1} that correspond to the assumed known parameters then invert the remaining matrix [13]:

$$C_{\tilde{\alpha}_1} = [I_{\tilde{\alpha}_1}]^{-1} \tag{14}$$

The second approach is to compute the CRB of the parameter vector α_1 subject to knowledge of the translation and rotation. To do so we compute an eigenvalue decomposition of I_{α_1}:

$$I_{\alpha_1} = [U_1 U_2] \begin{bmatrix} \Lambda_1 & 0 \\ 0 & 0 \end{bmatrix} \begin{bmatrix} U_1^T \\ U_2^T \end{bmatrix} \tag{15}$$

Except in degenerate cases (in which, for example, all sensors and at least one source signal are collinear), it can be shown that U_2 has 3 columns and that its columns span the subspace corresponding to overall scene translation and rotation. Then the constrained CRB of the parameter vector α_1 subject to knowledge of the translation and rotation is given by the pseudoinverse of I_{α_1} [14]:

$$\tilde{C}_\alpha = (I_\alpha)^\dagger = U_1 \Lambda_1^{-1} U_1^T \tag{16}$$

4.4 Partial Measurements

So far we have assumed that every sensor detects and measures both the TOA and DOA from every source signal. In this section we relax that assumption. We assume each emitted source signal is detected by only a subset of the sensors in the field and that a sensor that detects a source may measure the time-of-arrival (TOA) and/or the Direction-of-Arrival (DOA) for that source, depending on its capabilities. We denote the availability of a measurement using two indicator functions I_{ij}^t and I_{ij}^θ, where

$$I_{ij}^t, I_{ij}^\theta \in \{0, 1\} \tag{17}$$

If sensor i measures the TOA (DOA) for source j, then $I_{ij}^t = 1$ ($I_{ij}^\theta = 1$); otherwise, the indicator function is set to zero. Furthermore, let L denote the $2AS \times 1$ vector whose kth element is 1 if X_k is measured and is 0 if X_k is not measured; L is thus obtained by forming $A \times S$ matrices I^t and I^θ and stacking their column into a vector as in equation (1). Finally, define $\tilde{X}$ to be the vector formed from elements of X for which measurements are available, so X_k is in $\tilde{X}$ if $L_k = 1$.

The maximum likelihood estimator for the partial measurement case is similar to equation (12) but uses only those elements of X for which the corresponding element of L is one. Thus,

$$\hat{\alpha}_{1,ML} = \arg\min_{\alpha_1} \tilde{Q}(\tilde{X}; \alpha) \tag{18}$$

where (assuming uncorrelated measurement errors as in equation (11)),

$$\tilde{Q}(\tilde{X}; \alpha) = \sum_{i=1}^{A} \sum_{j=1}^{S} \left[\frac{(t_{ij} - \tau_{ij}(\alpha))^2}{\sigma_t^2} I_{ij}^t + \frac{(\theta_{ij} - \phi_{ij}(\alpha))^2}{\sigma_\theta^2} I_{ij}^\theta \right] \tag{19}$$

The Fisher Information Matrix for this case is similar to equation (13), but includes only information from available measurements; thus

$$\tilde{I}_{\alpha_1} = [\tilde{G}'(\alpha_1)]^T \Sigma^{-1} [\tilde{G}'(\alpha_1)] \tag{20}$$

where

$$\left[\tilde{G}'(\alpha_1)\right]_{ij} = L_i \cdot \frac{\partial \mu_i(\alpha_1)}{\partial (\alpha_1)_j} \tag{21}$$

We note that when partial measurements are available, the ML calibration may not be unique. For example, if only TOA measurements are available, a scene calibration solution and its mirror image have the same likelihoods. A complete understanding of the uniqueness properties of solutions in the partial measurement case is a topic of current research.

5. Numerical Results

We present some numerical examples of the self-calibration procedure. Ten sensor arrays and eleven sources are randomly placed in a $2\,\text{km}\times 2\,\text{km}$ region; the sensor orientations and source emission times are also randomly chosen. Figure 4 shows the locations of the sensors and sources. We assume every sensor detects each source emission and measures the TOA and DOA of the source. The measurement uncertainties are Gaussian with standard deviations of $\sigma_t = 1\,\text{msec}$ for the TOAs and $\sigma_\theta = 3^\circ$ for the DOAs. Neither the locations nor emission times of the sources are assumed to be known, and to eliminate the translation and rotation uncertainty in the scene, we assume either two sensors have known locations or one sensor has known location and orientation.

Figure 4 also shows the two standard deviation (2σ) location uncertainty ellipses for both the sources and sensors assuming the locations of sensor arrays $A1$ and $A2$ are known. These ellipses appear as small dots in the figure; an enlarged view for two sensors are shown in Figure 5. As a quantitative measure of performance, we compute for each sensor the equivalent 2σ uncertainty radius, defined as the geometric mean of the major and minor axis lengths of the 2σ uncertainty ellipse. We find that the average of the 2σ uncertainty radii for all ten sensors is $0.80\,\text{m}$ for this example.

Figure 6 shows a similar uncertainty plot, but in this case we assume that both the location and orientation of sensor $A1$ is known. In comparison with Figure 4, we see much larger uncertainty ellipses for the sensors, especially in the direction tangent to circles with center at sensor $A1$. The average 2σ uncertainty radius is $3.28\,\text{m}$ in this case. The high tangential uncertainty is primarily due to the DOA measurement uncertainty with respect to a known orientation of sensor $A1$. By comparing Figures 4 and 6, we see that it is more desirable to know the locations of two sensors than to know the location and orientation of a single sensor; thus, equipping two sensors with GPS systems results in lower uncertainty than equipping one sensor with a GPS and a compass.

Figure 7 shows the effect of increasing the number of sources on the average 2σ uncertainty radius. We plot the uncertainties found from using from 2 through 11 sources, starting initially with sources $S1$ and $S2$ and adding sources $S3$, $S4$, ... $S11$ at each step. We see the uncertainty reduces dramatically when the number of sources increases from 2 to 3 and then decreases more gradually as more sources are added. For this example, an average 2σ uncertainty radius of 1–3 meters is obtained when more than five signal sources are used for calibration.

The algorithms require low communication overhead as each sensor needs to communicate only $2S$ scalar values to the CIP. Computation of the calibration solution takes place at the CIP; for the examples presented the calibration computation takes on the order of 10 seconds using Matlab on a standard personal computer.

6. Conclusions

We have presented a procedure for calibrating the locations and orientations of a network of sensors. The calibration procedure uses source signals that are placed in the scene and computes array and source unknowns from estimated time-of-arrival and/or direction-of-arrival estimates obtained for each source-sensor pair. We present maximum likelihood solutions to four variations on this problem, depending on whether the source locations and signal emission times are known or unknown. We also discuss existence and uniqueness of solutions and algorithms for initializing the nonlinear minimization step in the maximum likelihood estimation. An analytical expression for the sensor location and orientation error covariance matrix is also presented for each of the four problem variations. A maximum likelihood calibration algorithm for the case of partial calibration measurements was also developed.

The algorithms require minimal communications from the sensors to a Central Information Processor, and computation of the calibration solution takes on the order of ten seconds using Matlab on a standard personal computer for examples considered.

Acknowledgement

This material is based in part upon work supported by the U.S. Army Research Office under Grant No. DAAH-96-C-0086 and Batelle Memorial Institute under Task Control No. 01092, and in part through collaborative participation in the Advanced Sensors Consortium sponsored by the U.S. Army Research Laboratory under the Federated Laboratory Program, Cooperative Agreement DAAL01-96-2-0001. Any opinions, findings, and conclusions or recommendations expressed in this publication are those of the authors and do not necessarily reflect the views of the U.S. Army Research Office, the Army Research Laboratory or the U.S. Government.

References

[1] N. Srour, "Unattended ground sensors a prospective for operational needs and requirements," tech. rep., Army Research Laboratory, October 1999.

[2] B. Friedlander and A. J. Weiss, "Direction Finding in the presence of Mutual Coupling," *IEEE Transactions on Antennas and Propogation*, vol. 39, pp. 273–284, 1991.

[3] N. Fistas and A. Manikas, "A New General Global Array Calibration Method," *IEEE Transactions on Acoustics, Speech and Signal Processing*, vol. 4, pp. 553–556, 1994.

[4] B. C. Ng and C. M. See, "Sensor-Array Calibration Using a Maximum-Likelihood Approach," *IEEE Transactions on Antennas and Propogation*, vol. 44, pp. 827–835, June 1996.

[5] J. Pierre and M. Kaveh, "Experimental Performance of calibration and direction-finding algorithms," in *Proceedings of the International Conference on Acoustics, Speech, and Signal Processing*, (Toronto, Canada), pp. 1365–1368, 1991.

[6] B. Flanagan and K. Bell, "Improved array self calibration with large sensor position errors for closely spaced sources," in *Proceedings of the First IEEE Sensor Array and Multichannel Signal Processing Workshop*, (Cambridge, MA), pp. 484 –488, March 2000.

[7] Y. Rockah and P. M. Schultheiss, "Array Shape Calibration Using Sources in Unknown Locations- Part II: Near-Field Sources and Estimator Implementation," *IEEE Transactions on Acoustics, Speech, and Signal Processing*, vol. 6, pp. 724–735, June 1987.

[8] E. R. Maniet, "Battlefield acoustic sensor calibration requirements," in *Proceedings of the 2000 Battlefield Acoustic and Seismic Sensing Meeting*, (Laurel, MD), pp. 339–344, October 17–19 2000.

[9] K. Yao, R. E. Hudson, C. W. Reed, D. Chen, and F. Lorenzelli, "Blind beamforming on a randomly distributed sensor array system," *IEEE Journal on Selected Areas in Communications*, vol. 16, pp. 1555–1567, October 1998.

[10] V. Cevher and J. H. McClellan, "Sensor array calibration via tracking with the extended kalman filter," in *Proceedings of the Fifth Annual Federated Laboratory Symposium on Advanced Sensors*, (College Park, MD), pp. 51–56, March 20–22 2001.

[11] J. Chaffee and J. Abel, "On the exact solutions of pseudorange equations," *IEEE Transactions on Aerospace and Electronic Systems*, vol. 30, pp. 1021–1030, October 1994.

[12] G. J. McLachlan and T. Krishnan, *The EM algorithm and extensions*. New York: Wiley, 1997.

[13] H. L. Van Trees, *Detection, Estimation, and Modulation Theory: Part I*. New York: Wiley, 1968.

[14] P. Stoica and T. L. Marzetta, "Parameter estimation problems with singular information matrices," *IEEE Transactions on Signal Processing*, pp. 87–90, January 2001.

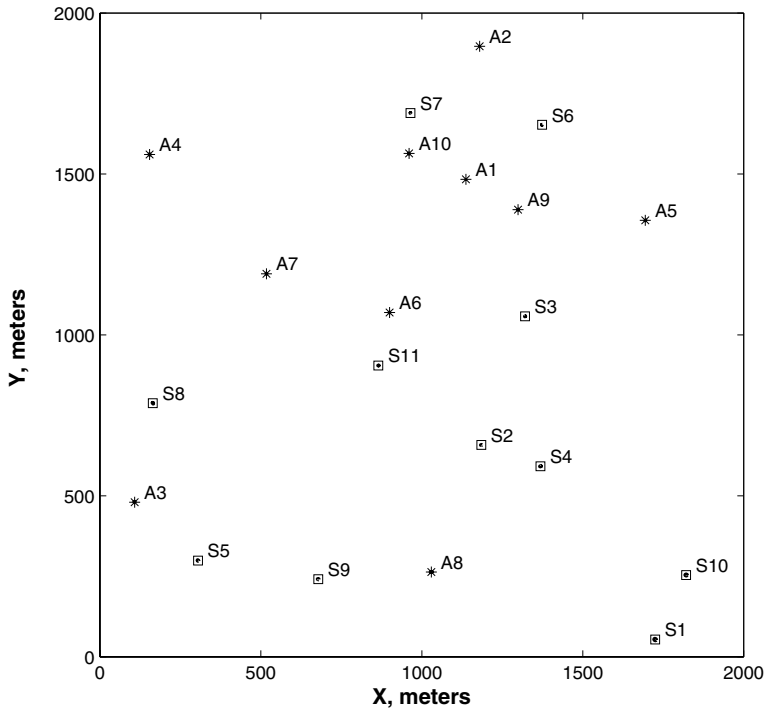

Figure 4: Example scene showing ten sensor arrays (stars) and eleven sources (squares). Also shown are the 2σ location uncertainty ellipses of the sensors and sources; these are on average less than 1 m in radius and show as small dots. The locations of sensors $A1$ and $A2$ are assumed to be known.

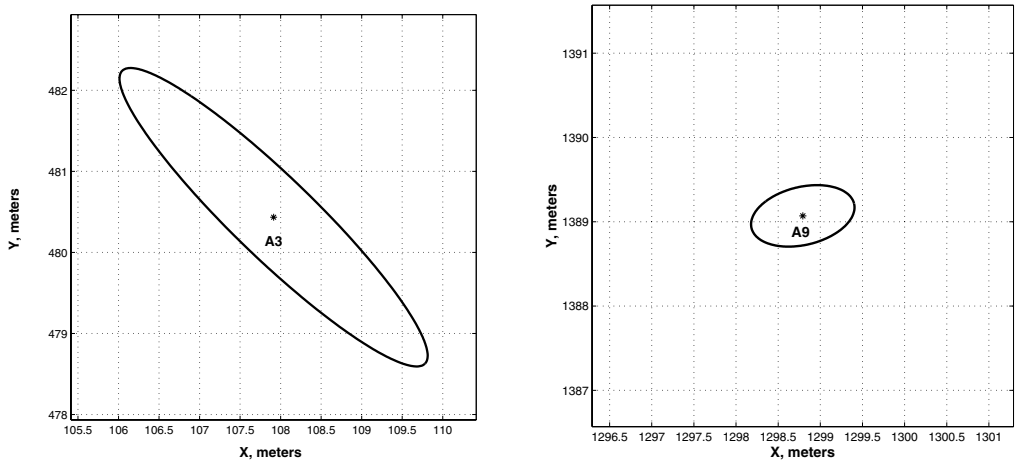

Figure 5: Two standard deviation location uncertainty ellipses for sensors $A3$ (left) and $A9$ (right) from Figure 4.

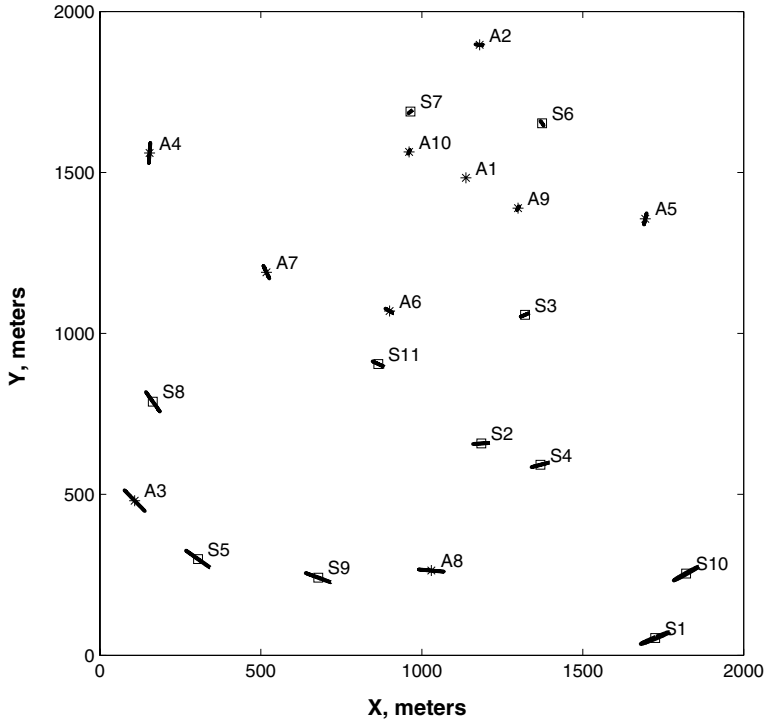

Figure 6: The 2σ location uncertainty ellipses for the scene in Figure 4 when the location and orientation of sensor $A1$ is assumed to be known.

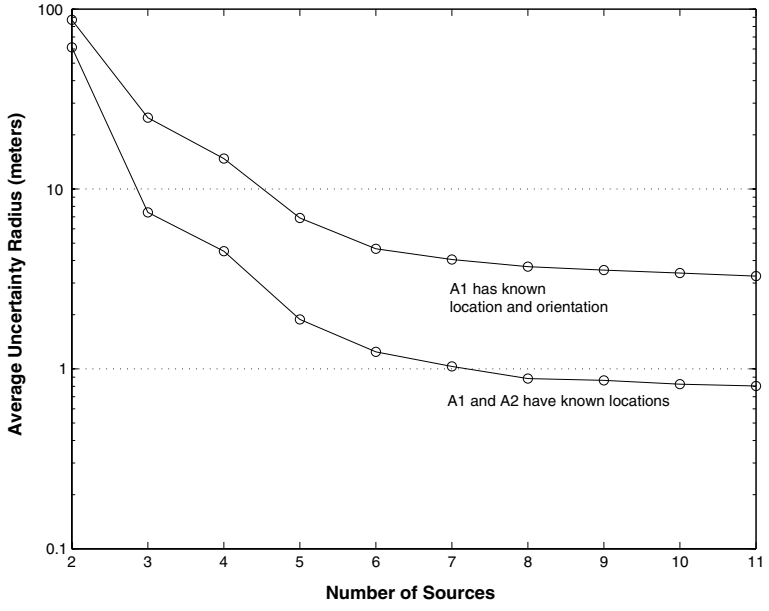

Figure 7: Average 2σ location uncertainty radius for the scenes in Figures 4 and 6 as a function of the number of source signals used.